Space Group Symmetry Fractionalization in a Chiral Kagome Heisenberg Antiferromagnet

Michael P. Zaletel, Zhenyue Zhu, Yuan-Ming Lu, Ashvin Vishwanath, and Steven R. White

Phys. Rev. Lett. **116**, 197203 — Published 11 May 2016

DOI: 10.1103/PhysRevLett.116.197203

Space group symmetry fractionalization in a chiral kagome Heisenberg antiferromagnet

Michael P. Zaletel,[1] Zhenyue Zhu,[2] Yuan-Ming Lu,[3] Ashvin Vishwanath,[4] and Steven R. White[2]

[1] *Station Q, Microsoft Research, Santa Barbara, California 93106-6105, USA*
[2] *Department of Physics and Astronomy, University of California, Irvine, Irvine, CA 92697, USA*
[3] *Department of Physics, The Ohio State University, Columbus, OH 43210, USA*
[4] *Department of Physics, University of California, Berkeley, California 94720, USA*

The anyonic excitations of a spin-liquid can feature fractional quantum numbers under space group symmetries. Detecting these fractional quantum numbers, which are analogs of the fractional charge of Laughlin quasiparticles, may prove easier than the direct observation of anyonic braiding and statistics. Motivated by the recent numerical discovery of spin-liquid phases in the kagome Heisenberg antiferromagnet, we theoretically predict the pattern of space group symmetry fractionalization in the kagome lattice SO(3)-symmetric chiral spin liquid. We provide a method to detect these fractional quantum numbers in finite-size numerics which is simple to implement in DMRG. Applying these developments to the chiral spin liquid phase of a kagome Heisenberg model, we find perfect agreement between our theoretical prediction and numerical observations.

Two-dimensional quantum spin liquids are distinguished by emergent excitations, 'spinons,' which carry a spin-1/2 moment, in striking contrast to all local excitations (e.g. magnons) which carry integer spin. Like the fractional charge of the Laughlin quasiparticles,[1] their spin is an example of 'symmetry fractionalization:' topological excitations can carry quantum numbers which are forbidden for local excitations. Wen proposed that in addition to charge and spin, the quantum numbers of space group (SG) symmetries, such as translations and rotations, could also become fractional. [2, 3] For example, roughly speaking a π-rotation could have a quantum number of $\pm i$ when acting on a topological excitation, while any local excitation has quantum number ± 1. Subsequent work revealed a zoo of gapped spin-liquid phases distinguished by the fractional SG quantum numbers of their excitations, which provide finer-grained invariants beyond their anyonic braiding and statistics. [2–10]

It is important to understand the type of symmetry fractionalization in a spin liquid since it provides one of the few potential experimental probes of fractionalized spin liquid physics. For example, SG fractionalization has spectroscopic signatures,[2, 3, 11] and determines the nearby ordered phases that are connected to the spin liquid via continuous phase transitions.[5, 12–15] Great theoretical progress has been made in classifying the possible patterns of SG symmetry fractionalization,[7, 9] though it has yet to be detected in a Heisenberg spin model.[16]

Here we report the direct numerical detection of SG symmetry fractionalization in a Heisenberg antiferromagnet on the kagome lattice. Recently it was discovered that introducing chiral symmetry breaking terms [17, 18] or further-neighbor exchange interactions [19–22] can stabilize a chiral spin liquid (CSL). Proposed by Kalmeyer and Laughlin, the CSL is the magnetic analog of the $\nu = \frac{1}{2}$ bosonic quantum Hall effect, with a robust spin-carrying gapless edge.[23–25] The CSL contains a single type of anyonic excitation, the $S = 1/2$ spinon 's,'

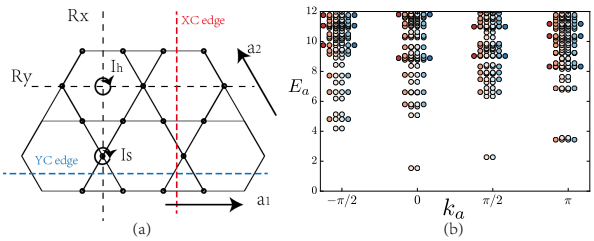

FIG. 1. **a**) Symmetry operations and two typical edges in numerical studies of the kagome chiral spin liquid. **b**) Entanglement spectrum $\{E_a\} = -\log(\rho_L)$ of the YC8 s-sector, plotted against the momentum k_a around the cylinder. The lowest pair is a 'Kramers doublet' under the anti-unitary R_x, indicating $(R_x^2)_s = -1$. Since the pair occur at the same T_1 momentum, $(R_x T_1)^2 = -1$ as well, as expected from $(R_x T_1)_s^2 = -1$.

which has semionic self-statistics. In close analogy to the Laughlin flux-threading argument, when 2π-flux of the S^z spin rotation is thread through the system, the flux nucleates a spinon s. Since s carries $S^z = \pm\frac{1}{2}$ itself, the flux insertion has induced spin, which is the famous spin-Hall response $\sigma_{xy}^{\text{spin}} = \pm\frac{1}{2}$. The sign of the response depends on the parity-breaking chirality.

Previous studies have confirmed fractionalization of SO(3)-symmetry in the kagome CSL, which can be inferred from the fractional spin-Hall response[21]. In this work, we theoretically predict the pattern of SG symmetry fractionalization in an SO(3)-symmetric kagome CSL, and develop a numerical framework for detecting SG fractionalization using the ground states obtained from cylinder DMRG. Surprisingly, we prove that only a single fractionalization pattern is possible for an SO(3)-symmetric kagome CSL, in sharp contrast to the many possibilities in a $\mathbb{Z}_2$ spin-liquid [5, 13]. SG symmetries are not simple to probe in 'snake' DMRG, [26] since the chosen 1D ordering of the sites breaks the SG symmetries. We introduce a technique, the 'classical product state (CPS)

trick,' for detecting SG symmetry fractionalization. The CPS trick also drastically simplifies the measurement of the topological S and T matrices,[27] which previously required Monte Carlo sampling as expensive as the DMRG itself.[28] Using both finite and infinite DMRG on the J_1-J_2-J_3 Heisenberg model, we find perfect agreement with theoretical predictions. The methods introduced here are applicable to many other spin liquid models.

Theory of symmetry fractionalization in a CSL.

In addition to SO(3) rotations of spins, the kagome model has SG symmetries illustrated in Fig. 1. $T_{1,2}$ denote translations along Bravais vectors $\mathbf{a}_1, \mathbf{a}_2$, and C_6 is a hexagon-centered $\pi/3$ rotation. In particular there are two inequivalent inversion operations: hexagon-centered $I_h = (C_6)^3$, and site-centered $I_s = T_1 I_h$. Both reflection symmetry and time-reversal are spontaneously broken by the chiral order parameter of the CSL. However, their combination is preserved, so we define *anti*-unitary reflections R_x, R_y, whose orientation with respect to the Bravais vectors is illustrated in Fig. 1. The SG generators satisfy the algebraic conditions summarized in the left column of Tab. I, where $\boldsymbol{e}$ represents the identity element. Throughout, cylinder types are labeled as in Ref. [29].

The symmetry fractionalization[2, 7, 9] of the CSL is encoded in how symmetry operations act on individual spinons. For example, when the inversion I_h acts on a spinon, it may acquire a phase '$\pm i$,' which is 'fractional' since on local objects $I_h = \pm 1$. Other symmetry-group relations can be similarly fractionalized, which we tabulate in Tab. I. In each case, there is a group relation that should produce the identity (like $I_h^2 = \boldsymbol{e}$) which instead produces a phase, i.e., the spinon carries a 'projective' representation. There is a constraint on the phase: since a pair of spinons annihilates to the vacuum, $s \times s = \mathbb{1}$, and the vacuum can't be fractionalized, the phases are $\mathbb{Z}_2$-valued, ± 1. The phase factors associated with the last two algebraic identities in Tab. I, however, are not well-defined, because one can redefine T_1, T_2 by the $\mathbb{Z}_2$ factors $T_i \to \pm T_i$, changing the phase factor. [2, 7, 9] In contrast, for the first six relations such a redefinition cancels, so these six $\mathbb{Z}_2$-valued phase factors are the symmetry fractionalization invariants of a CSL on the kagome lattice.

We now derive the symmetry fractionalization of the CSL and a set of concrete measurements to detect it. In general, there can be several possible symmetry fractionalization patterns consistent with a particular anyon model, and it is an energetic question which pattern happens to be realized (this is the case for the time-reversal symmetric $\mathbb{Z}_2$ spin-liquid, for example). For the CSL, however, we will prove there is actually a *unique* possible pattern so long as SO(3)-symmetry is preserved. We do so by first determining how each of the invariants can be measured from the degenerate ground states of a long (or infinite) cylinder,[30] and then constraining these measurements on general grounds.

Algebra	Fractionalization	Measurements
$T_1T_2T_1^{-1}T_2^{-1} = \boldsymbol{e}$	-1	$e^{\mathrm{i}(P_s - P_{\mathbb{1}})}$
$(C_6)^6 = (I_h)^2 = \boldsymbol{e}$	-1	$Q_s(I_h)/Q_{\mathbb{1}}(I_h)$
$(R_x)^2 = \boldsymbol{e}$	-1	R_x-SPT on YC8
$(R_y)^2 = \boldsymbol{e}$	-1	R_y-SPT on XC8
$R_xT_1R_x^{-1}T_1 = \boldsymbol{e}$	$+1$	R_xT_1-SPT on YC8
$R_xT_2R_x^{-1}T_2^{-1}T_1 = \boldsymbol{e}$	-1	R_yT_y-SPT on XC8
$C_6T_1{C_6}^{-1}T_2^{-1} = \boldsymbol{e}$	$+1$ (gauge fixing)	N/A
$C_6T_2{C_6}^{-1}T_2^{-1}T_1 = \boldsymbol{e}$	$+1$ (gauge fixing)	N/A

TABLE I. Each group relation (left column) can be fractionalized when acting on a spinon, producing a phase ± 1 we have predicted for the kagome CSL (middle column). The first two invariants can be measured from global SG quantum numbers, while the anti-unitary reflection invariants R_x, R_y require measuring 1D-SPT invariants. The last two relations are not invariant under redefinitions of the generators by ± 1, so do not produce meaningful invariants.

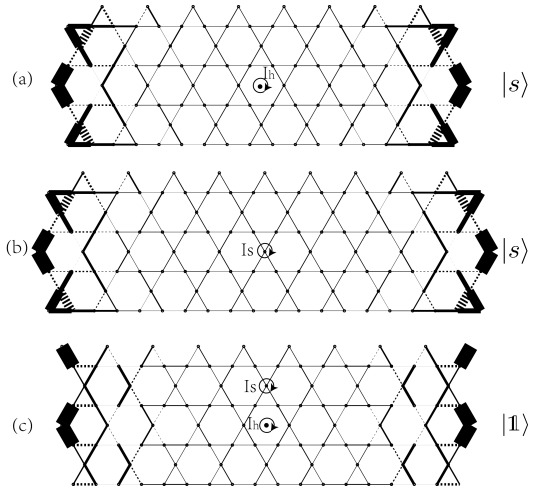

FIG. 2. Finite DMRG geometries used for XC8. Geometries (a) and (b) have an odd number of edge spins, trapping a spinon, from which we compute $Q_s(I_h), Q_s(I_s)$. From (c), we compute both $Q_{\mathbb{1}}(I_h)$ and $Q_{\mathbb{1}}(I_s)$. The results are tabulated Fig. 3. A similar set of geometries is used for YC8, whose edge differs by 90-degrees.

Consider, for example, the relation $(I_h^2)_s = -1$. Measuring such a phase would seem to be a contradiction, since when I_h acts on a finite number of spins it must give ± 1 by its very definition. The key insight is that rather than trying to act with I_h on a single spinon, we create a pair of spinons related by I_h, and measure the global I_h quantum number of the pair. Strictly speaking, we are interested in their quantum number relative to that of the vacuum. If -1, it is as if $I_h \cdot s = \pm i \cdot s$ when acting on each spinon individually, which indicates fractionalization. The robustness of this procedure was argued in Ref. [30].

In practice, it is not necessary to actually nucleate

and manipulate a spinon pair. Instead, we make use of topological ground state degeneracy. Like a torus, an infinitely long cylinder has a two-fold ground state degeneracy. A useful basis choice are the minimally entangled states (MES),[27, 31, 32] which are labeled by the two topological 'sectors' $\{|\mathbb{1}\rangle, |s\rangle\}$. These states have definite topological flux $\mathbb{1}/s$ threading the cylinder, and given the state $|\mathbb{1}\rangle$, the state $|s\rangle$ is obtained by nucleating a pair of spinons and separating them out to infinity. If we instead use a finite cylinder (Fig. 2) the pair eventually encounters the boundaries; since we must leave one at each edge, there is a energy splitting between $|\mathbb{1}\rangle, |s\rangle$, but this is purely a boundary effect. The ratio of I_h quantum numbers $Q_{\mathbb{1}/s}(I_h)$ in these two states reveals the fractionalization of the spinon: $\frac{Q_s(I_h)}{Q_{\mathbb{1}}(I_h)} = (I_h)_s^2$.

We now prove that $(I_h^2)_s = -1$ for a CSL, so long as SO(3) is preserved, using the flux-fusion test introduced in Refs. 33 and 34. The spinon sector $|s\rangle$ can be obtained from the vaccum state $|\mathbb{1}\rangle$ by adiabatically threading S^z-flux ϕ through the cylinder, i.e., by twisting the boundary conditions. Due to the spin-Hall response, when $\phi = 2\pi$, $\Delta S^z = \pm\frac{1}{2}$ of spin has been transferred from one end of the cylinder; this should be interpreted as the spinon sector $|s\rangle$, since the spinons brought to the edge bring with them a magnetic moment. The S^z flux ϕ will be inverted ($\phi \to -\phi$) by either inversion I_h or π spin rotation $e^{\mathrm{i}\pi S^x}$, but (with a proper choice of branch cut) it will remain invariant under their combination $e^{\mathrm{i}\pi S^x} I_h$. Therefore we can track the eigenvalue of $e^{\mathrm{i}\pi S^x} I_h$ throughout the flux insertion process, which must remain unchanged:

$$\frac{Q_s(e^{\mathrm{i}\pi S^x} I_h)}{Q_{\mathbb{1}}(e^{\mathrm{i}\pi S^x} I_h)} = 1 = \left[(e^{\mathrm{i}\pi S^x} I_h)^2\right]_s \tag{1}$$

As noticed in Ref. 34, to be compatible with the SO(3) spin rotational symmetry, a plaquette-centered inversion operation must commute with all spin rotations when acting on the semionic spinons. Therefore we have

$$\left[(e^{\mathrm{i}\pi S^x} I_h)^2\right]_s = (e^{\mathrm{i}2\pi S^x})_s \cdot (I_h^2)_s = 1. \tag{2}$$

Since each semion carries spin-1/2, $(e^{\mathrm{i}2\pi S^x})_s = -1$, proving that $(I_h^2)_s = -1$.

We next turn to lines 3-6 in Tab. I. The fractionalization invariant $(R_x^2)_s = \pm 1$ encodes whether the spinon carries such a 'Kramers degeneracy' under the anti-unitary reflection R_x. To detect it, consider a YCn cylinder on which R_x does not exchange the two edges. As shown in Refs. [30, 35, 36], each ground state sector can formally be regarded as a gapped 1D spin chain characterized by 1D symmetry protected topological (SPT) invariants.[37–39] The reflection $G = \mathbb{Z}_2^{R_x}$ is analogous to 'on-site time-reversal,' which has a $\mathbb{Z}_2$ SPT invariant '$\{+1, -1\}$'. The trivial phase $(+1)$ typically has gapped edges, while the nontrivial SPT phase (-1) has degenerate edge states which are a 'Kramers pair' under R_x, with $R_x^2 = -1$, analogous to a spin-1 Haldane chain. By measuring the R_x-SPT invariant of $|s\rangle$ relative to $|\mathbb{1}\rangle$, we can check for Kramers degeneracy of the spinon.

We prove that $(R_x^2)_s = -1$ for any CSL whose spinons carry half-integer spin. Since S^z flux ϕ adiabatically inserted through the cylinder is invariant under the combined operation of spin rotation $e^{\mathrm{i}\pi S^x}$ and R_x,[40] the $\mathbb{Z}_2$ 1D-SPT invariant associated with the anti-unitary symmetry $e^{\mathrm{i}\pi S^x} R_x$ must remain constant as $|\mathbb{1}\rangle \to |s\rangle$, implying

$$\left[(e^{\mathrm{i}\pi S^x} R_x)^2\right]_s = (e^{\mathrm{i}2\pi S^x})_s \cdot (R_x^2)_s = 1. \tag{3}$$

As a result we have $R_x^2 = -1$ for spin-1/2 semions.

We find that the remaining four invariants can be measured and theoretically predicted in a similar fashion, which we leave to the SI. Consequently all the invariants summarized in Tab. I are fixed.

Absolute quantum numbers. We have predicted the relative quantum numbers between topological sectors, but under certain assumptions the absolute quantum numbers can be predicted as well. Consider a cylinder whose ground state has no free moments, i.e., $\langle \mathbf{S}_i \rangle = 0$ on all sites. If the ground state remains moment-free when adding a pair of spins to the lattice, one at each edge, the introduced moments must be 'screened' by pair creation of spin-1/2 excitations, i.e., spinons, which sit precisely on the additional sites. Note that the spin-1/2 character of the added sites was essential, otherwise a *local* excitation could screen the new moment. As the entire cylinder can be built up this way, the lattice behaves like a crystal of semionic spinons.

We assume that the global quantum number I_h of the geometry can be computed by taking this picture literally and applying I_h to each pair of spinons (i.e., sites). This assumption is true within the parton construction, [30, 41] but we contend it holds more generally. Under I_h the spinon on each lattice site exchanges with its inversion counterpart, and meanwhile each spinon also rotates by π around itself. Due to the semionic statistics of spinons, each counter-clockwise exchange will contribute a phase $e^{\mathrm{i}\pi/2}$ per inversion-related pair, while counter-clockwise self-rotation by π leads to phase $e^{\mathrm{i}\pi/4}$ per spinon. During this exchange, the trajectory of each pair always encloses an even number of the other semions, so there is no further statistical phase. Therefore the total phase obtained in this process is

$$Q(I_h) = e^{\mathrm{i}\frac{\pi}{2}\frac{N_s}{2}} \cdot e^{\mathrm{i}\frac{\pi}{4}N_s} = (-1)^{\frac{N_s}{2}} = (-1)^{\#\text{ of } I_h\text{-pairs}}, \tag{4}$$

where N_s denotes the total number of lattice sites. This prediction has a nontrivial dependence on the cylinder type, since on XC8, the central column contains a single pair of sites, while on YC8, it contains two.

When computing I_s, two contributions differ. First, two of the sites are left invariant, so they do not acquire a phase. Second, the exchange of all the remaining pairs encloses *one* of these stationary sites, acquiring an extra

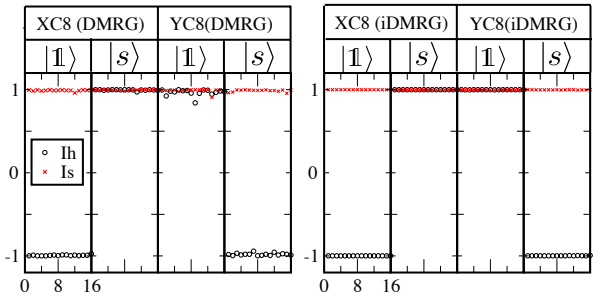

FIG. 3. The measured reflection quantum numbers $Q_{\mathbb{1}/s}(I_{h/s})$ inferred from 16 CPS overlaps $a_\sigma/a_{I_{h/s}\sigma}$. Results were obtained using both finite and infinite DMRG on YC8 and XC8 cylinders.

mutual statistics $(-1)^{N_s/2-1}$. Together,

$$Q(I_s) = (-1)^{\#\text{ of } I_s\text{-pairs}} \cdot (-1)^{\#\text{ of } I_s\text{-pairs}} \equiv +1. \quad (5)$$

Numerically detecting symmetry fractionalization: the CPS trick. If one had access to the wave function as a dense vector—as in exact diagonalization—it would be trivial to compute the needed global quantum numbers. However, DMRG maps the cylinder to a 1D chain and then compresses the wave function as a matrix product state (MPS). A symmetry operation $\hat{U}$ mapping sites to sites can be written as a (long) product of nearest neighbor swap operators. One can then, in principle, calculate the symmetry overlap $Q_U = \langle\Psi|\hat{U}|\Psi\rangle$ by sequentially applying the swaps to $|\Psi\rangle$ and doing a final MPS-MPS overlap calculation. In practice, the intermediate states produced when applying the swaps can have more entanglement than the ground state itself, requiring bigger bond dimensions, and this method is rather slow and unsatisfactory.

A better approach involves measuring the overlap of $|\Psi\rangle$ against several random classical product states ('CPS'). The wavefunction can be expanded in a complete basis of CPS $\{\sigma\}$, $|\Psi\rangle = \sum_\sigma a_\sigma |\sigma\rangle$. If $\hat{U}|\Psi\rangle = Q_U|\Psi\rangle$, then $a_{U\sigma} = Q_U a_\sigma$, where $U\sigma$ is another CPS trivially obtained from σ. Thus a single pair of CPS amplitudes, a_σ and $a_{U\sigma}$, are enough to determine Q_U. In practice, since $|\Psi\rangle$ is approximate, we obtain a distribution $Q_U(\sigma)$ with mean $\langle\Psi|\hat{U}|\Psi\rangle$, and if $|\Psi\rangle$ is accurate the distribution is sharply peaked at the correct value. In order to ensure that a_σ is non-negligible, the configurations $\{\sigma\}$ are efficiently sampled according to the probability distribution $|\Psi|^2$. [42] In contrast to a calculation time of $O(Nm^3)$ for a DMRG sweep, where N is the number of sites and m is the bond dimension, sampling each CPS requires only $O(Nm^2)$ operations, so thousands of samples can be collected in the same time as a single DMRG sweep. In practice we find only a handful are required.

Similarly, while in principle it is known how to measure 1D-SPT invariants in infinite DMRG [43], the existing algorithm is cumbersome in the case where the reflection permutes the DMRG snake, requiring swaps of cost m^3. We find a CPS trick can be used to measure the 1D-SPT invariants of an infinite cylinder at cost m^2, as detailed in the SI. The CPS trick can be extended to other measurements that require SG operations. For example, in order to compute the topological S and T matrices [27] given the degenerate ground states of a torus $\{|a\rangle\}$, one must compute overlaps of the form $\langle b|\hat{R}_\theta|a\rangle$ where R_θ is a rotation of the torus. In the SI we show the result can be trivially computed from a handful of CPS overlaps at cost $\mathcal{O}(m^2)$.

Results. We study the CSL phase at $J_1 = 1.0$, $J_2 = J_3 = 0.5$ using complex wavefunctions, so that time-reversal symmetry is spontaneously broken. We computed the inversion quantum numbers on XC8 and YC8 cylinders using both finite[44, 45] and infinite DMRG.[46, 47] In finite DMRG, the topological sector is switched from $|\mathbb{1}\rangle$ to $|s\rangle$ by adding a site at each end of the cylinder,[29] as illustrated in Fig. 2, which attracts a spinon to each edge for energetic reasons. In infinite DMRG, the two sectors appear as a ground state degeneracy.[28, 48] Given the ground state, the global I_h/I_s quantum numbers were measured using the CPS trick, with a typical set of samples shown in Fig. 3. There is little noise, indicating $|\Psi\rangle$ is very nearly symmetric. In all cases, the relative quantum numbers $Q_s/Q_{\mathbb{1}}$ are in agreement with predictions. Furthermore, recall that for YC8 geometries in the vacuum, we predicted $(-1)^{\#\text{ of } I_h\text{-pairs}} = 1$, while for XC8 $(-1)^{\#\text{ of } I_h\text{-pairs}} = -1$. This difference is reflected in the observed absolute quantum numbers.

To measure $(R_x^2)_s$, we measured the $\mathbb{Z}_2$ 1D-SPT invariant associated with R_x using iDMRG. The result, $(R_x^2)_s = -1$, is apparent from the entanglement spectrum of the $|s\rangle$ sector, shown in Fig. 1. The same Kramers degeneracy predicted to occur at the edge will also appear in the entanglement spectrum between the left and right halves of the cylinder. As seen in Fig. 1, the spectrum indeed has a two-fold degeneracy which was verified (see SI) to transform as an R_x-Kramers doublet; the $|\mathbb{1}\rangle$ sector, in contrast, does not. Both levels occur at the same momentum around the cylinder, meaning T_1 acts trivially on the doublet, so the pair is also a Kramers doublet under R_xT_1, implying $(R_xT_1)_s^2 = -1$. Similar agreement for R_y was found on XC8.

In conclusion, we have shown that the kagome CSL has a unique but non-trivial pattern of SG symmetry fractionalization, and detected this pattern in a microscopic Heisenberg kagome model. In addition, we have elucidated a general framework for probing SG symmetries with DMRG which can be applied to other recently discovered spin liquid phases. The nearest-neighbor Heisenberg kagome model, for example, may be a $\mathbb{Z}_2$ spin-liquid, which has many possible symmetry fractionalization patterns. However, for the cylinder circumferences currently

in reach with DMRG, it has not been possible to identify all the required degenerate ground states, so at present we are unable to measure all the SG quantum numbers required to uniquely identify the fractionalization pattern.[30]

We thank D Huse for many discussions and his ongoing contributions to related work. MPZ acknowledges helpful conversations with L Cincio and M Cheng. YML is supported by the startup funds at Ohio State University. AV is supported by the Templeton Foundation and by a Simons Investigator grant. SRW and ZZ acknowledge support from the NSF under grant DMR-1505406 and from the Simons Foundation through the Many Electron collaboration. Note added: After the initial completion of this paper, we became aware of a related work.[49]

[1] R. B. Laughlin, Phys. Rev. Lett. **50**, 1395 (1983).
[2] X.-G. Wen, Phys. Rev. B **65**, 165113 (2002).
[3] X.-G. Wen, Phys. Rev. D **68**, 065003 (2003).
[4] A. Kitaev, *January Special Issue*, Annals of Physics **321**, 2 (2006).
[5] F. Wang and A. Vishwanath, Phys. Rev. B **74**, 174423 (2006).
[6] Y.-M. Lu, Y. Ran, and P. A. Lee, Phys. Rev. B **83**, 224413 (2011).
[7] A. M. Essin and M. Hermele, Phys. Rev. B **87**, 104406 (2013).
[8] A. Mesaros and Y. Ran, Phys. Rev. B **87**, 155115 (2013).
[9] M. Barkeshli, P. Bonderson, M. Cheng, and Z. Wang, ArXiv e-prints (2014), arXiv:1410.4540 [cond-mat.str-el].
[10] S. Bieri, L. Messio, B. Bernu, and C. Lhuillier, Phys. Rev. B **92**, 060407 (2015).
[11] A. M. Essin and M. Hermele, Phys. Rev. B **90**, 121102 (2014).
[12] S. Sachdev, Phys. Rev. B **45**, 12377 (1992).
[13] Y.-M. Lu and Y. Ran, Phys. Rev. B **84**, 024420 (2011).
[14] Y.-M. Lu, G. Y. Cho, and A. Vishwanath, ArXiv e-prints (2014), arXiv:1403.0575 [cond-mat.str-el].
[15] Y.-M. Lu, ArXiv e-prints (2015), arXiv:1505.06495 [cond-mat.str-el].
[16] H. Song and M. Hermele, Phys. Rev. B **91**, 014405 (2015).
[17] M. Greiter, D. F. Schroeter, and R. Thomale, Phys. Rev. B **89**, 165125 (2014).
[18] B. Bauer, L. Cincio, B. Keller, M. Dolfi, G. Vidal, S. Trebst, and A. Ludwig, Nat Commun **5**, (2014).
[19] L. Messio, B. Bernu, and C. Lhuillier, Phys. Rev. Lett. **108**, 207204 (2012).
[20] Y. C. He, D. Sheng, and Y. Chen, Phys. Rev. Lett. **112**, 137202 (2014).
[21] S.-S. Gong, W. Zhu, and D. Sheng, Scientific reports **4** (2014).
[22] A. Wietek, A. Sterdyniak, and A. M. Laeuchli, Phys. Rev. B **92**, 125122 (2015).
[23] V. Kalmeyer and R. B. Laughlin, Phys. Rev. Lett. **59**, 2095 (1987).
[24] X. G. Wen, F. Wilczek, and A. Zee, Phys. Rev. B **39**, 11413 (1989).
[25] M. Greiter and R. Thomale, Phys. Rev. Lett. **102**, 207203 (2009).
[26] E. Stoudenmire and S. R. White, Annual Review of Condensed Matter Physics **3**, 111 (2012).
[27] Y. Zhang, T. Grover, A. Turner, M. Oshikawa, and A. Vishwanath, Phys. Rev. B **85**, 235151 (2012).
[28] L. Cincio and G. Vidal, Phys. Rev. Lett. **110**, 067208 (2013).
[29] S. Yan, D. A. Huse, and S. R. White, Science **332**, 1173 (2011).
[30] M. Zaletel, Y.-M. Lu, and A. Vishwanath, ArXiv e-prints (2015), arXiv:1501.01395 [cond-mat.str-el].
[31] A. Kitaev and J. Preskill, Phys. Rev. Lett. **96**, 110404 (2006).
[32] S. Dong, E. Fradkin, R. G. Leigh, and S. Nowling, Journal of High Energy Physics **2008**, 016 (2008).
[33] M. Hermele and X. Chen, ArXiv e-prints (2015), arXiv:1508.00573 [cond-mat.str-el].
[34] Y. Qi, M. Cheng, and C. Fang, ArXiv e-prints (2015), arXiv:1509.02927 [cond-mat.str-el].
[35] M. P. Zaletel, Phys. Rev. B **90**, 235113 (2014).
[36] C.-Y. Huang, X. Chen, and F. Pollmann, Phys. Rev. B **90**, 045142 (2014).
[37] F. Pollmann, A. M. Turner, E. Berg, and M. Oshikawa, Phys. Rev. B **81**, 064439 (2010).
[38] L. Fidkowski and A. Kitaev, Phys. Rev. B **83**, 075103 (2011).
[39] X. Chen, Z.-C. Gu, and X.-G. Wen, Phys. Rev. B **84**, 235128 (2011).
[40] Note that the location of the twist boundary condition requires one to choose a 'defect line' whose location breaks R_x; thus the symmetry $e^{\mathrm{i}\,\pi S^x} R_x$ implicitly includes a 'gauge-transformation' $e^{i\phi S^z}$ on a subset of the spins in order to bring the defect line back to the same position. This transformation doesn't change any of the relevant group relations.
[41] Y. Qi and L. Fu, Phys. Rev. B **91**, 100401 (2015).
[42] E. M. Stoudenmire and S. R. White, New Journal of Physics **12**, 055026 (2010).
[43] F. Pollmann and A. M. Turner, Phys. Rev. B **86**, 125441 (2012).
[44] S. R. White, Phys. Rev. Lett. **69**, 2863 (1992).
[45] Finite DMRG calculations were performed using ITensor library: http://itensor.org/.
[46] I. P. McCulloch, (2008), arXiv:0804.2509.
[47] J. A. Kjäll, M. P. Zaletel, R. S. K. Mong, J. H. Bardarson, and F. Pollmann, Phys. Rev. B **87**, 235106 (2013).
[48] M. P. Zaletel, R. S. K. Mong, and F. Pollmann, Phys. Rev. Lett. **110**, 236801 (2013).
[49] L. Cincio and Y. Qi, (2015), arXiv:1511.02226.